Experimental and Numerical Element Tests for Granular Soils: Performance of Different Constitutive Models for Monotonous and Low-Cycle Loading

Stefanie Danne and Achim Hettler

Abstract It is known that some common constitutive models show deficits when predicting elastic and plastic deformations due to high- and low-cycle loading resulting for example from geotechnical installation processes. The object of part I of subproject 8 within the DFG research group FOR 1136 (GeoTech) is to show the performance of different constitutive models and to compare them to experimental laboratory test results and among each other. To look onto the incremental stress–strain behaviour of sand, series of drained, stress-controlled triaxial tests have been carried out to obtain strain response envelopes for monotonous loading. Here, a soil element is subjected to a constant stress increment in different directions and its strain responses are evaluated graphically. The presented laboratory tests were performed at different initial stress states. The accumulation of strains due to low cyclic loading ($N \leq 50$) has also been examined for different loading directions and different sizes of stress amplitudes. All experiments have been recalculated numerically with different constitutive models, amongst them some common as well as advanced constitutive models, which have been developed recently and partly within the research group GeoTech.

Keywords Low-cycle loading · Triaxial tests · Strain response envelopes · Incremental stress–strain behaviour · Granular soils

S. Danne (✉) · A. Hettler
Chair of Soil Mechanics and Foundation Engineering, Technical University
of Dortmund, Dortmund, Germany
e-mail: stefanie.danne@tu-dortmund.de

1 Introduction

In practical applications, soil elements can be subject to monotonous as well as to stress or strain cycles with different magnitudes of amplitudes. Constitutive equations used to solve boundary value problems should generally be able to model all these loading situations and predict resulting stresses and deformations realistically.

Especially, when it comes to cyclic loading, occurring for example during geotechnical installation processes, it is well known that some common constitutive models show deficits when predicting elastic and plastic deformations with regard to magnitude as well as to accumulation.

In general, cyclic loading processes can be divided into high-cycle and low-cycle loading, depending on the number of cycles N. To avoid numerical errors and high computing time, it is often useful to calculate deformations due to high-cycle loading by means of explicit models, where irreversible strains are treated similar to creep deformations under constant loads [14]. In Wichtmann's High Cycle Accumulation model, the strain amplitudes are limited to $\Delta\varepsilon \leq 10^{-3}$. So it is appropriate to use other constitutive equations for low number of cycles, where the magnitude of strains is often $\geq 10^{-3}$. Low-cycle loading processes can be defined for a lower number of cycles with $N \leq 50$, [4]. In these cases, an implicit calculation of deformations is often appropriate.

After describing some fundamentals in Sect. 2 of this paper, numerical and experimental analyses of monotonous and low-cycle loading in triaxial testing are presented. The results of different monotonous loading paths are evaluated by means of response envelopes in Sect. 3. In Sect. 4, the stress–strain behaviour during low-cycle loading is examined, where the focus is set on the accumulation of plastic strains. A comprehensive study of quasi-elastic strains during low-cycle loading can be found in [5].

By comparing the experimental and numerical results, an attempt is made to show the performance of some common and advanced constitutive models.

2 Fundamentals

2.1 Response Envelopes

In axial symmetric conditions considered in this paper, index 1 denotes the axial component and index 3 the lateral component of stress or strain, respectively. The stress ratio η is defined by the quotient of the deviatoric stress $q = \sigma_1 - \sigma_3$ and the mean pressure $p = (\sigma_1 + 2\sigma_3)/3$ describing the stress state's position in the p–q plane.

To avoid distortion of two vectors in the p–q plane, which are orthogonal to each other in the three-dimensional principal stress space $\sigma_1 - \sigma_2 - \sigma_3$, stresses and strains in this paper are presented in the Rendulic plane, which is isomorphic. Its horizontal axis is $\sqrt{2}\sigma_3$ and $\sqrt{2}\varepsilon_3$, respectively, and the vertical axis σ_1 and ε_1 (Fig. 1).

So-called response envelopes are a useful tool for calibrating, validating and comparing constitutive equations [11]. The soil's incremental stress–strain behaviour can hereby be investigated during first loading as well as during un- and reloading processes. First basics of response envelopes were presented in the 1970s by [12]. A few years later, [9] used this concept in context with the development of constitutive equations.

To obtain a response envelope, a soil element is subjected to a certain stress or strain increment. Considering the concept of *strain*-response envelopes dealt with in this paper—subsequently referred to as "SREs"—a constant stress increment

$$\Delta\sigma = \sqrt{\Delta\sigma_1^2 + 2\Delta\sigma_3^2} \tag{1}$$

is applied in different directions α_σ, Fig. 1a.

The corresponding "response" of the soil in terms of either strain or stress is determined and presented graphically. The direction of the implied stress or strain increment with a constant absolute value is varied and leads to different stress or strain responses, endpoints of which are connected to a response envelope.

The strains are also plotted in the isomorphic rendulic diagram, in which the resulting total strain increment is

$$\Delta\varepsilon = \sqrt{\varepsilon_1^2 + 2\Delta\varepsilon_3^2} \tag{2}$$

The angles α_σ and α_ε shown in Fig. 1 are used herein to quantify the direction of incremental quantities. α_σ is the angle between stress probe vector and the positive $\sqrt{2}\sigma_3$-axis and α_ε is the angle between the strain increment vector and the positive $\sqrt{2}\varepsilon_3$-axis.
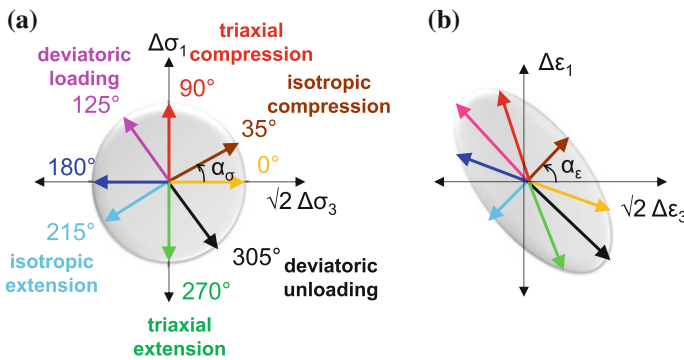
Fig. 1 Applied stress increments $\Delta\sigma$ (**a**) and corresponding strain responses (**b**) for different directions α_σ

Table 1 Initial stress states

Stress state	p (kPa)	q (kPa)	Stress-ratio $\eta = q/p$ [−]	Region
A	200	150	0.75	Compression
I	200	0	–	Isotropic
J	200	−100	−0.5	Extension

2.2 Triaxial Device and Testing Procedure

The triaxial device used for experiments presented in this paper is equipped with high-resolution measurement and control technology. The confining pressure as well as the axial force can be controlled independently, so that stress paths in different directions from any initial stress state can be performed.

The tested soil is a fine-grained sand with a low uniformity-index ($C_U = 1.25$, $d_{50} = 0.15$ mm), having a positive impact when it comes to avoid effects from membrane penetration. Height and diameter of the soil specimen are 10 cm.

The soil sample was fabricated by pluviating dry sand thereby maintaining a constant height. This specimen-preparation method was kept constant for all tests. The achieved relative densities I_D were well reproducible with small deviation (± 0.1). Starting with an isotropic stress, the predefined initial stress state was reached, either by increasing the vertical stress (for stress states in compression) or the horizontal stress (for stress states in extension). Then the soil sample was consolidated.

The experiments described in this paper are carried out with medium to dense soil samples ($I_D \approx 0.75$), consolidated at initial stress states shown in Table 1.

For all experiments and stress probe directions, one equally prepared and consolidated sample is used. The stress-controlled experiments are carried out under drained conditions. The rate and the frequency during low-cycle loading, respectively, are kept low to avoid pore water pressure. All stresses referred to in this paper are effective stresses ($\sigma = \sigma'$).

2.3 Considered Constitutive Equations

There are quite some constitutive models for granular soils, which are used to calculate boundary value problems for practical purposes. It is known, however, that some of them show deficits when predicting deformations due to high- and/or low-cycle loading processes.

In this paper, some of them are chosen exemplarily to compare them with each other and to the experiments, which have been carried out by the authors. The constitutive equations are

- Hypoplasticity with intergranular strain (IS);
- Hardening Soil model (HS);
- Intergranular Strain Anisotropy-model (ISA);
- Simple Anisotropic Sand Plasticity model (Sanisand).

The **hypoplastic constitutive model** describes the stress–strain behaviour of non-cohesive soils in rate form. Its present version was formulated by von Wolffersdorff [20]. Small strain stiffness formulation (so-called intergranular strain concept) was added by [13].

The **Hardening Soil model** developed by [16] is formulated in the framework of classical theory of plasticity. Total strains are calculated using a stress-dependent stiffness, different for first loading and un-/reloading. Plastic strains are calculated by introducing a multi-surface yield criterion. Hardening is assumed to be isotropic depending on both the plastic shear and the volumetric strain. For the frictional hardening, a non-associated and for the cap hardening an associated flow rule is assumed.

The elastoplastic **ISA model** recently introduced by [8] is based on the intergranular strain concept, but contrary to the existing formulations it proposes a yield function describing a surface within the intergranular strain space. It includes an elastic locus in the intergranular strain space.

The **Sanisand model** was developed within the framework of critical state soil mechanics and bounding surface plasticity [17]. As analytical description of a narrow but closed cone-type yield surface, which obeys rotational and isotropic hardening, an 8-curve equation is used.

The numerous material parameters needed for the different constitutive models for the used fine sand have either been determined experimentally by the authors or have been kindly provided by colleagues of the Karlsruhe Institute of Technology (KIT).

3 Experimental and Numerical Results from Monotonous Loading

To obtain a SRE from monotonous loading, once a chosen initial stress state is reached and consolidation is finished, and a stress path in one direction is applied until failure, Fig. 2.

Total strains $\Delta \varepsilon$ are evaluated for different stress increments $\Delta \sigma = 20, 30, 40, 50$ and 100 kPa (circles in Fig. 2a). The same procedure is repeated with an equally prepared new sample.

(a)

(b)
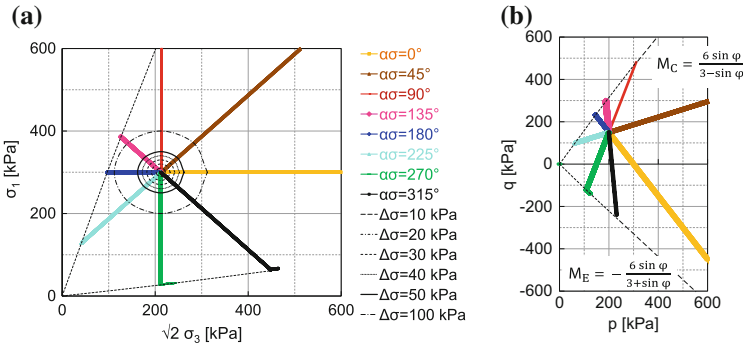
Fig. 2 Applying monotonous stress probes (here from stress state *A*) in the Rendulic plane (**a**) and in the *p*–*q* plane (**b**)

3.1 Experimental Results

There are few papers which report of experimental SREs for momentous loading, e.g. [1, 3, 6]. An overview can be found in [5].

Figure 3 shows SREs determined experimentally for three different initial stress states, Table 1.

For all stress states, it turns out that the size of the SREs non-linearly increases with increasing stress increment. It can also be seen that the SREs derived from stress states in extension (Fig. 3a) and compression (Fig. 3c) get longer and slimmer, the closer the stress increment approaches the failure lines shown in Fig. 2. Largest deformations occur for pure deviatoric loading ($\alpha_\sigma \approx 125°$) for the initial stress state located in compression and for deviatoric unloading ($\alpha_\sigma \approx 305°$) for the initial stress state located in extension.

For the stress state located on the isotropic axis (*I*), the shapes of the strain response envelopes for $\Delta\sigma \leq 50$ kPa are almost similar to symmetrical ellipses. For larger stress increments, the envelope becomes elongated towards extension region.

3.2 Numerical Results

The experiments described in Sect. 3.1 have been recalculated numerically with the aforementioned constitutive equations.

Figure 4 shows the numerically determined SREs for initial stress state *A* (compression). Except for the Sanisand model, the SREs' elongation and inclination are in good agreement with the experimental results shown in Fig. 3c. Regarding the size of the SREs, only the hypoplastic model seems to depict the adequate stiffness.

Figure 5 shows the numerically determined SREs for the isotropic initial stress state *I*. Approximate symmetrical envelopes for $\Delta\sigma \leq 50$ kPa can be found at the HS
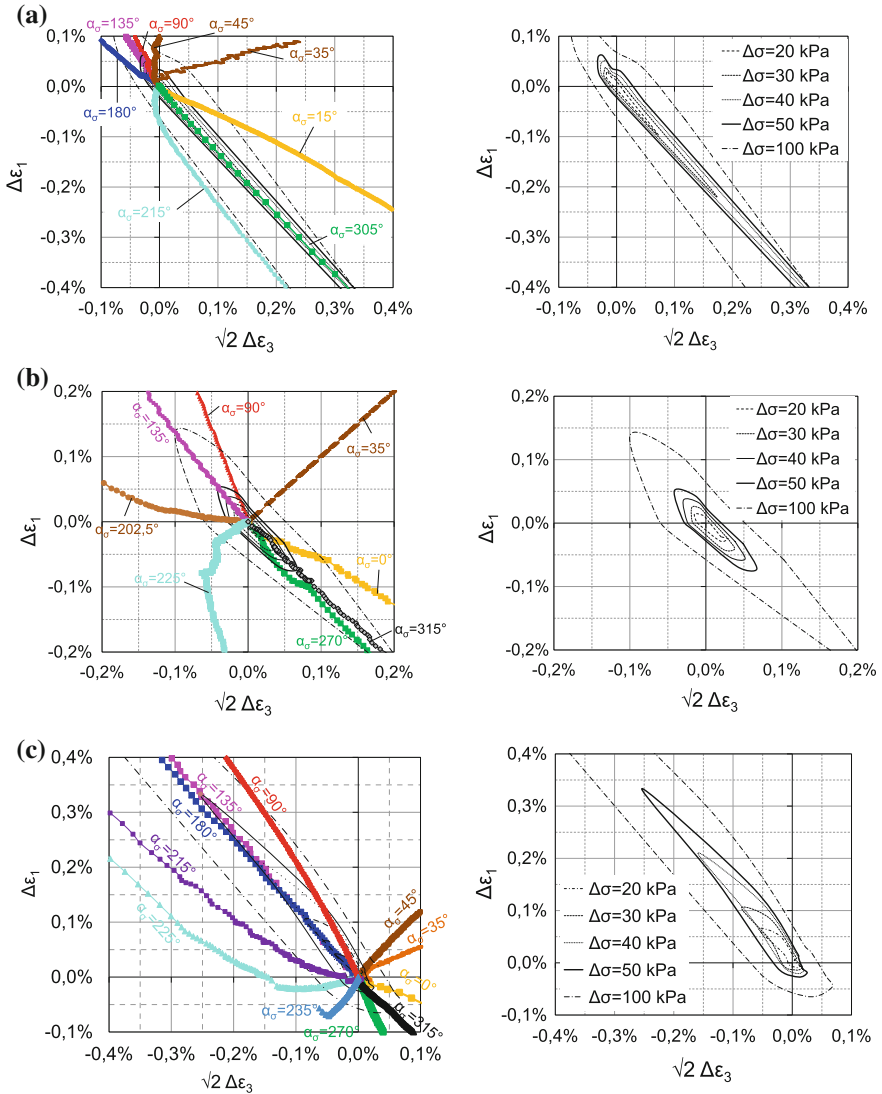
Fig. 3 Strain response envelopes for initial stress states A (**a**), I (**b**) and J (**c**)

and the Sanisand model, which is in good agreement with the experimental results shown in Fig. 3b.

For the SREs calculated from stress state J shown in Fig. 6, a significant difference between un- and reloading stress probes can be observed for the hypoplastic model (Fig. 6a). For isotropic unloading ($\alpha_\sigma \approx 215°$), the resulting strains are very small and lead to an asymmetrical shape of the envelopes. The elastoplastic SREs in

(a)

(b)

(c)

(d)
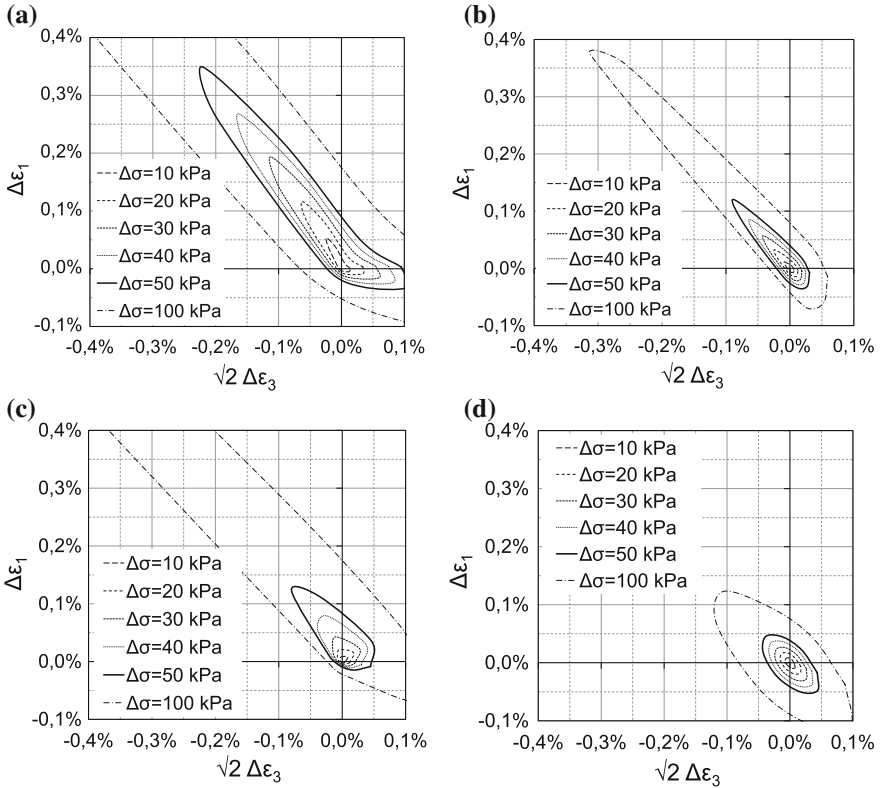
Fig. 4 Numerically determined SREs at initial stress state *A*: **a** Hypoplasticity (with IS), **b** Hardening Soil, **c** ISA, **d** Sanisand

Fig. 6b, d are quite similar but here again smaller, i.e. stiffer than the SREs obtained experimentally.

Numerical investigations of (other) different constitutive equations and their evaluation and comparison by means of SREs can be found in [2, 7, 15, 19].

4 Experimental and Numerical Results from Low-Cycle Loading

The strain accumulation during low-cycle loading has also been examined in this paper. Exemplarily, the results for different stress cycles with two different increment sizes each are presented in this paper:

- pure deviatoric loading ($\alpha_\sigma \approx 125°$): $\Delta q = 50$ kPa and $\Delta q = 200$ kPa with $\Delta p = 0$ and
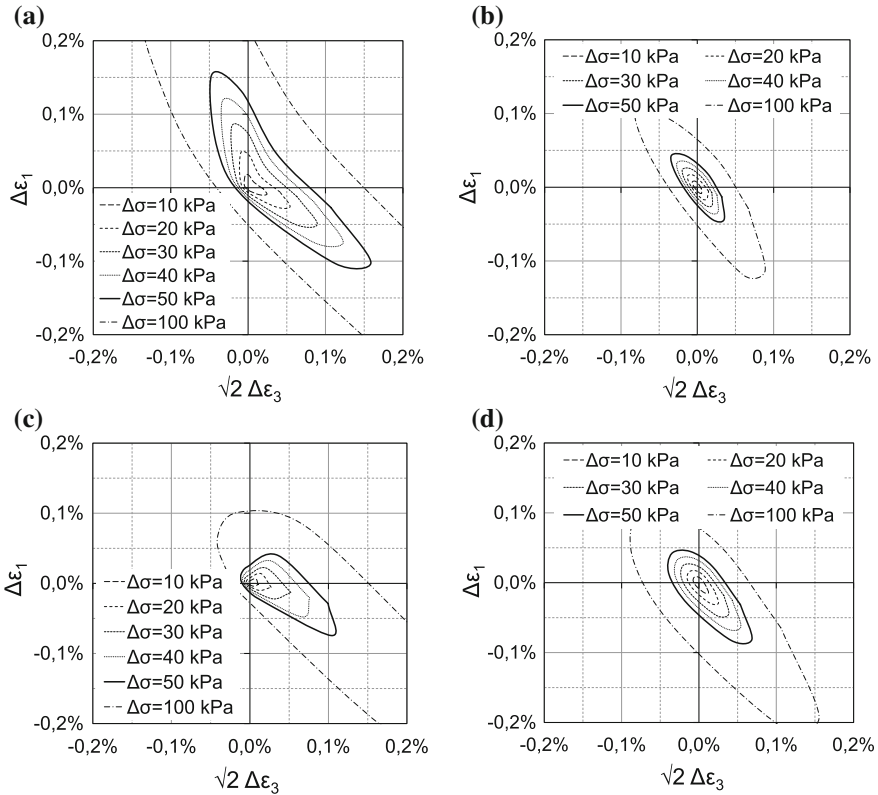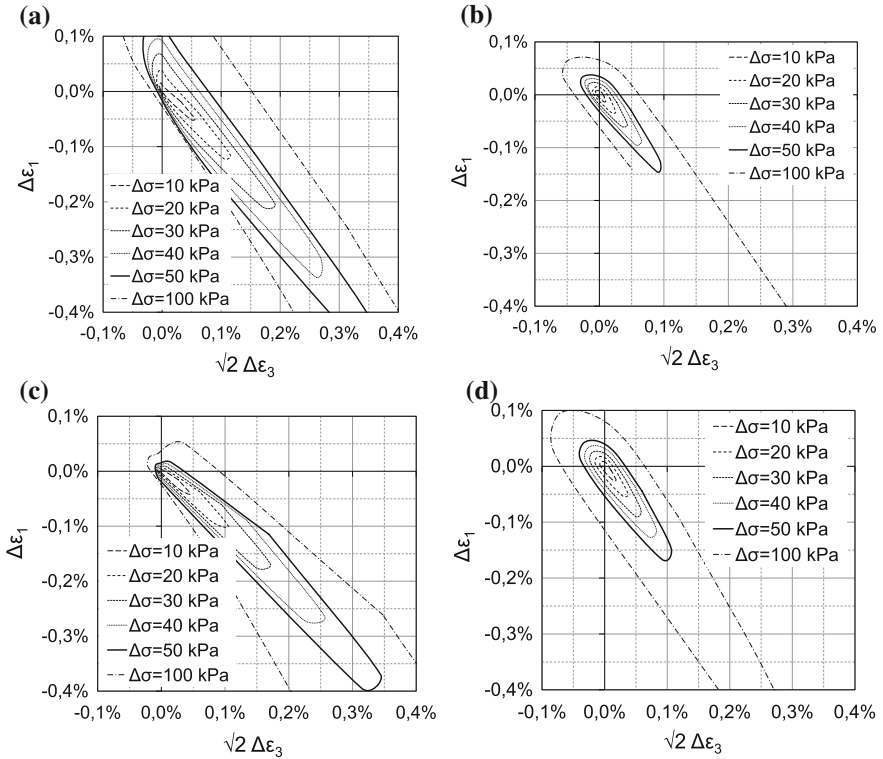
Fig. 5 Numerically determined SREs at initial stress state I: **a** Hypoplasticity (with IS), **b** Hardening Soil, **c** ISA, **d** Sanisand

- pure volumetric loading ($\alpha_\sigma \approx 35°$): $\Delta p = 50$ kPa and $\Delta p = 200$ kPa with $\Delta q = 0$

The cycles are applied on a soil specimen/element, starting from the isotropic stress state I (Table 1). The results are presented by plotting the total strains $\Delta\varepsilon$ over the number of cycles N.

In each case both increment sizes for the same direction are plotted in one figure. The solid lines show the total strains $\Delta\varepsilon$ during 20 cyclic stress increments of 200 kPa (magnitudes shown on the left axis of ordinates), and the dashed lines show the development of total strains during smaller stress cycles of 50 kPa (magnitudes shown on the right axis of ordinates).

Fig. 6 Numerically determined SREs at initial stress state J: **a** Hypoplasticity (with IS), **b** Hardening Soil, **c** ISA, **d** Sanisand

4.1 Experimental Results

The experimental results are shown in Fig. 7. Both loading directions show that the largest strain increase occurs during first loading. Another similarity which attracts attention is the fact that after a few cycles, already the quasi-elastic strain, i.e. the difference between $\Delta\varepsilon_{\text{loading}} - \Delta\varepsilon_{\text{unloading}}$, seems to be constant and independent from the number of cycles N. Generally, the total and the quasi-elastic strains due to pure deviatoric loading (Fig. 7a) are larger than for an isotropically loaded soil element (Fig. 7b). A logarithmic increase of total strains can be observed here, which still slightly continues after 20 stress cycles.

In contrast to deviatoric loading, there is quasi-elastic behaviour for isotropically loaded samples after a low number of cycles already. In this case, no further increase of strains can be observed. For high-cycle loading, an increase may be noticeable for a large number of cycles ($N \gg 50$), see e.g. [18].
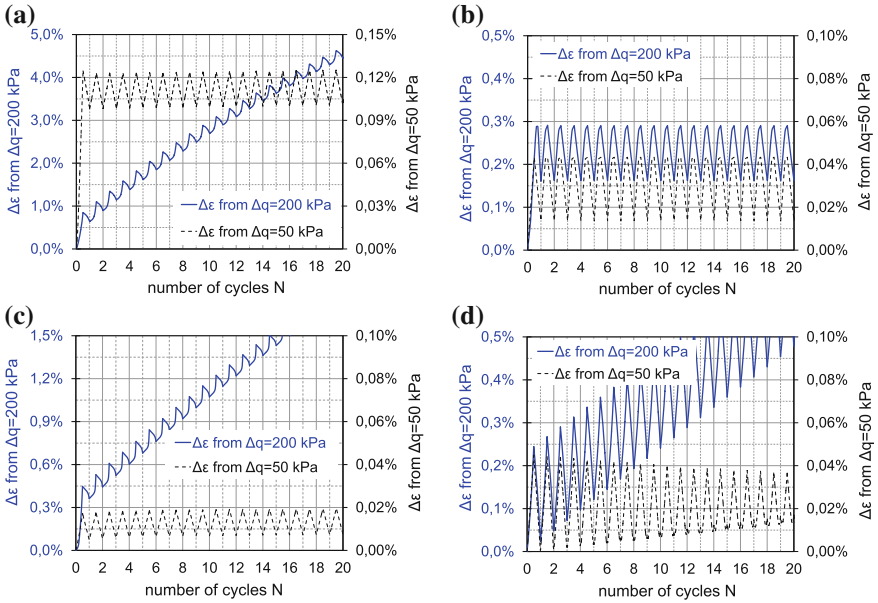
Fig. 7 Strain accumulation during 20 pure deviatoric stress cycles (**a**) and pure isotropic stress cycles (**b**)
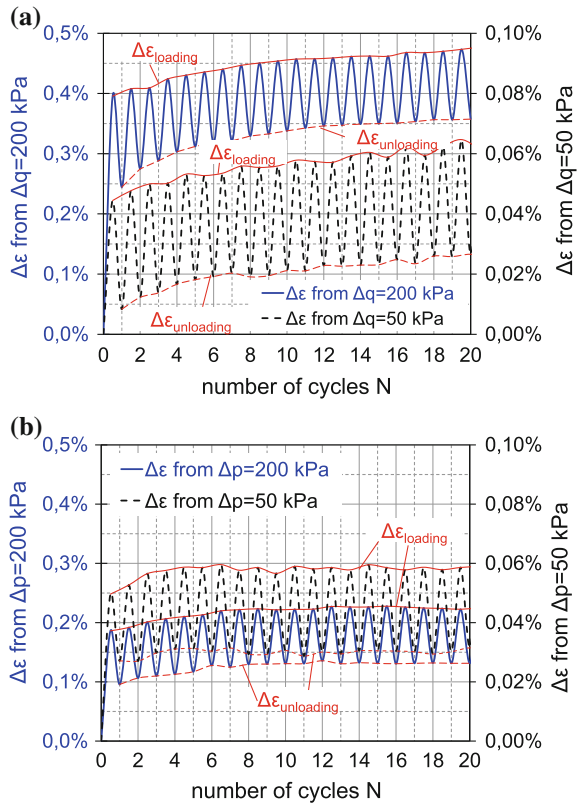

4.2 Numerical Results

Figures 8 and 9 show the strain accumulation of the corresponding numerical calculations.

It can be observed that there is no strain accumulation at all after the second un- and reloading for the calculations carried out with the elastoplastic HS model, Figs. 8b and 9b. The largest strains are obtained for the calculations with the hypoplastic model for both deviatoric and volumetric loading conditions. While the strains due to $\Delta q = 50$ kPa seem to be almost elastic after the second un- and reloading, ratcheting occurs during larger stress cycles with $\Delta q = 200$ kPa, Fig. 8a. For large volumetric stress cycles in Fig. 9a this ratcheting-effect becomes significantly smaler, so that the calculated total strains for this loading direction are in good agreement to the experimental results shown in Fig. 7b. Fuente's ISA model provides an increasing tendency of strains for both amplitudes, and their magnitudes, however, seem to be either too large ($\Delta q = 200$ kPa) or too small ($\Delta q = 50$ kPa), Fig. 8c. The Sanisand model shows a constant strain increase with each $\Delta q = 200$ kPa-cycle, for $\Delta q = 50$ kPa there even seems to be a decrease of total and elastic strains.

Fig. 8 Strain accumulation during 20 pure deviatoric stress cycles: **a** Hypoplasticity (with IS), **b** Hardening Soil, **c** ISA, **d** Sanisand
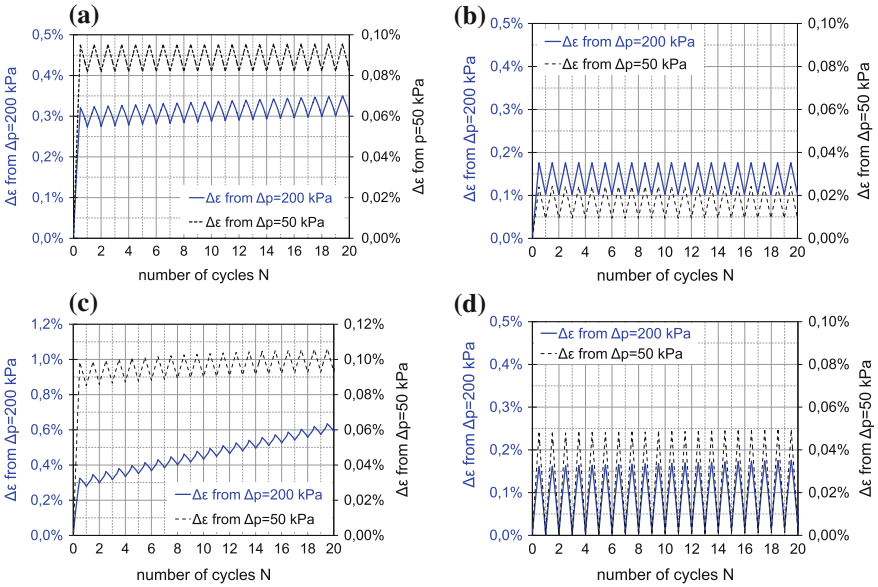
Fig. 9 Strain accumulation during 20 pure volumetric stress cycles: **a** Hypoplasticity (with IS), **b** Hardening Soil, **c** ISA, **d** Sanisand

Figure 9 shows the strain accumulation of the corresponding numerical calculations for pure volumetric stress cycles.

The results in this case are qualitatively in agreement with the ones from pure deviatoric un- and reloading.

5 Summary and Further Hints

When comparing the numerical and experimental results presented in this paper, fairly good agreements could be found considering monotonous loading.

Considerable differences, however, have been found when investigating the development of total and quasi-elastic strains during low-cycle loading. None of the four investigated constitutive models were able to simulate the strains for the investigated loading directions close to the experimental results. This means further research work is needed to improve existing incremental stress–strain relations. Especially, for low-cycle loading it is recommended to check thoroughly the stress paths dominating the actual boundary value problem and to choose a suitable constitutive model.

References

1. Anandarajah, A., Sobhan, K., Kuganenthira, N.: Incremental stress-strain behaviour of granular soil. J. Geotech. Eng.—ASCE **121**(1), 57–68 (1995)
2. Calvetti, F., Viggiani, G., Tamagnini, C.: A numerical investigation of the incremental behaviour of granular soils. Rivista Italiana di Geotecnica 11–19 (2003)
3. Costanzo, D., Viggiani, G., Tamagnini, C.: Directional response of a reconstituted fine-grained soil—Part I: Experimental investigation. Int. J. Numer. Anal. Meth. Geomech. **13**, 1283–1301 (2006)
4. Danne, St., Hettler, A.: Verhalten von nichtbindigen Böden bei niederzyklischer Belastung. Geotechnik **36**, 19–29 (2013)
5. Danne, St., Hettler, A.: Experimental strain response-envelopes of granular materials for monotonous and low-cycle loading processes. In: Holistic Simulation of Geotechnical Installation Processes—Numerical and Physical Modelling. Lecture Notes in Applied and Computational Mechanics (77). Springer International Publishing, 229–250 (2015)
6. Doanh, T.: Strain response envelope: a complementary tool for evaluating hostun sand in triaxial compression and extension: experimental observations. In: Constitutive Modelling of Granular Materials. Springer, Berlin, 375–396 (2000)

7. Froiio, F., Roux, J.-N.: Incremental response of a model granular material by stress probing with DEM simulations. In: IUTAM-ISIMM Symposium on Mathematical Modelling and Physical Instances of Granular Flow, Reggio Calabria, Italy (2009)
8. Fuentes Lacouture, W.M.: Contributions in mechanical modelling of fill materials. Veröffentlichung des Institutes für Bodenmechanik und Felsmechanik am Karlsruher Institut für Technologie (KIT) (2014)
9. Gudehus, G.: A comparison of some constitutive laws for soils under radially symmetric loading and unloading. In: Wittke, W. (Ed.), Proceedings of the 3rd International Conference on Numerical Methods in Geomechanics, Balkema, 1309–1323 (1979)
10. Hettler, A., Danne, St.: Strain response envelopes for low-cycle loading processes. In: Proceedings of the 18th International Conference on Soil Mechanics and Geotechnical Engineering, Paris, 1491–1494 (2013)
11. Kolymbas, D.: Response-Envelopes: A useful tool, aus "Hypoplasticity then and now". In: Kolymbas, D. (ed.) Constit. Modell. Gran. Mater. 57–105. Springer-Verlag, Berlin (2000)
12. Lewin, P., Burland, J.: Stress-probe experiments on saturated normally consolidated clay. Géotechnique **20**(1), 38–56 (1970)
13. Niemunis, A., Herle, I.: Hypoplastic model for cohesionless soils with elastic strain range. Mech. Cohesive-Frictional Mater. **2**, 279–299 (1997)
14. Niemunis, A., Wichtmann, T., Triantafyllidis, T.: A high-cycle accumulation model for sand. Comput. Geotech. **32**(4), 245–263 (2005)
15. Royis, P., Doanh, T.: Theoretical analysis of strain response envelopes using incrementally non-linear constitutive equations. Int. J. Numer. Anal. Meth. Geomech. **22**(2), 97–132 (1998)
16. Schanz, T., Vermeer, P.A., Bonnier, P.G.: 1999. The hardening soil model: Formulation and verification. Beyond 2000 in Computational Geotechnics—10 Years of Plaxis. Balkema, Rotterdam (2000)
17. Taiebat, M., Dafalias, Y.: Sanisand, simple anisotropic sand plasticity model. Int. J. Numer. Anal. Meth. Geomech. **32**(8), 915–948 (2008)
18. Triantafyllidis, Th., Wichtmann, T., Niemunis, A.: Entwicklungen in der Bodenmechanik, Bodendynamik und Geotechnik. In: Dr.-Ing. Frank Rackwitz (Ed.) Festschrift zum 60. Geburtstag von Univ.-Professor Dr.-Ing. habil. Stavros A. Savidis, 173–191 (2006)
19. Tamagnini, C., Masın, D., Costanzo, D., Viggiani, G.: An evaluation of different constitutive models to predict the directional response of a reconstituted fine-grained soil. Modern Trends in Geomechanics, Springer, Berlin Heidelberg New York **106**, 143–157 (2006)
20. von Wolffersdorff, P.-A.: A hypoplastic relation for granular materials with a predefined limit state surface. Mech. Cohesive-Frictional Mater. **1**, 251–271 (1996)